

SOUTH AMERICAN MONSOON DURING THE TWO PHASES OF THE PACIFIC DECADAL OSCILLATION

Sâmia R. Garcia*; Mary T. Kayano**

Instituto Nacional de Pesquisas Espaciais, São José dos Campos, SP, Brazil

1. INTRODUCTION

Monsoon system is the major component of the summer rainfall over some continental areas. This system develops over low latitude lands in response to seasonal thermal contrast between continents and the adjacent oceanic regions. The climate over a large portion of South America (SA) shows monsoon characteristics, among others the wet summer and dry winter (Vera *et al.*, 2005; Grimm *et al.*, 2004). The South American Monsoon system (SAMS) interannual variability is related to the El Niño/Southern Oscillation (ENSO). However, the PDO might also influence the SAMS variability.

Decadal variations and long-term trends have been found for hydrometeorological parameters in SA. Zhou and Lau (2001) obtained a decadal mode of summer rainfall with opposite sign anomalies over northwestern and northeastern SA for 1979-1995. Several authors found increased rainfall over the Amazon basin during 1980-1990 relative to 1950-1960 (e.g., Chu *et al.*, 1994). Andreoli and Kayano (2005) found larger

magnitudes of El Niño related summer negative rainfall anomalies over northwestern SA for warm than for cold PDO phase.

The multi-decadal variability of the monsoon systems is not well understood. Thus, the present paper examines further the decadal variability of the SAMS considering several variables.

2. DATA AND METODOLOGY

The data used consist of monthly gridded sea surface temperature (SST) and reanalyzed surface air temperature, 200 hPa velocity potential (χ), 500 hPa vertical velocity, sea level pressure (SLP) and precipitable water (PW) fields. The SST data are the extended reconstructed SST at 2° by 2° latitude-longitude resolution grid for 1854-2000 (Smith and Reynolds, 2003). The reanalyzed data in the global area between 80°N and 80°S for 1948-1999 are obtained from the National Centers for Environmental Prediction (NCEP) (Kalnay *et al.*, 1996).

Accordingly to Tanaka *et al.* (2004), the Hadley circulation component is contained in the zonal means of χ ; and the Walker and monsoon components, in the deviations from these means, ($\chi^*(t, x, y)$), where x , y , and t are longitude, latitude and time, respectively. They also assumed that the Walker circulation is included in the annual mean of $\chi^*(t, x, y)$ and defined the monsoon circulation as the deviations from the

Corresponding authors address: Instituto Nacional de Pesquisas Espaciais, Centro de Previsão de Tempo e Estudos Climáticos, São José dos Campos, SP, Brasil.
E-mails: *samia@cptec.inpe.br,
**mary@cptec.inpe.br

annual mean of $\chi^*(t, x, y)$, referred here to as $\chi^{*'}(t, x, y)$ or transient- χ .

Monthly anomalies of $\chi^{*'}(t, x, y)$ are calculated using climatologies of partial and total periods. Monthly anomalies of SST, surface air temperature, SLP, 500 hPa vertical velocity, and PW are computed at each grid point as departures from the 1948-1999 means. The anomaly series at each grid point are standardized by the corresponding standard deviation (σ).

The dominant modes for the transient- χ anomaly field in the South American area bounded at 10°N, 40°S, 120°W and 10°W are obtained subjecting this variable to EOF analysis. Separated EOF analyses are done for partial and total periods, considering year-round monthly data. The method proposed by North et al. (1982) is used to test the physical meaningful identity of the modes. The eigenvectors are presented as correlation patterns. To assess the statistical significance of these correlations, the number of degrees of freedom (DOF) is estimated for each mode by dividing the principal component (PC) length by the time interval of two independent realizations in the PC series. The Student t-test with a confidence level of 95% is then used.

Composite cases are selected from seasonally averaged PC time series for summer (December to February - DJF) and winter (from June to August - JJA). Thresholds of $\pm 0.5\sigma$ of the seasonal PC01 of 1948-1999 are used. The negative (positive) composite includes cases with PC01 $< -0.5\sigma$ ($> 0.5\sigma$). The statistical significance of the composites is assessed considering the DOF as the number of years included in each composite. The Student t-test is applied using a confidence level of 95%.

3. RESULTS

3.1 SAMS dominant modes

The EOF01 and EOF02 of the transient- χ anomalies for 1948-1976 are well separated from each other and explain 53.3% and 26.4% of the total variance for this variable, respectively. The EOF01 presents the largest loadings with a southeast-northwest orientation over SA (Fig. 1a). For positive (negative) PC01, 200 hPa convergence (divergence) occurs over SA. This mode describes interannual variability superimposed to decadal variability in some periods (Fig. 1b). Indeed, positive PC01 values

prevail from 1958 to 1965, and the negative ones after 1972.

The PC02 time series shows interannual oscillations with periods approximately of 4-5 years (Fig. 1d). For positive (negative) PC02, the divergent (convergent) flow over eastern tropical Pacific compensates the convergent (divergent) flow over northeastern Brazil and tropical Atlantic (Figs. 1c and 1d). Thus, the EOF02 illustrates ENSO related pattern for transient- χ anomaly field.

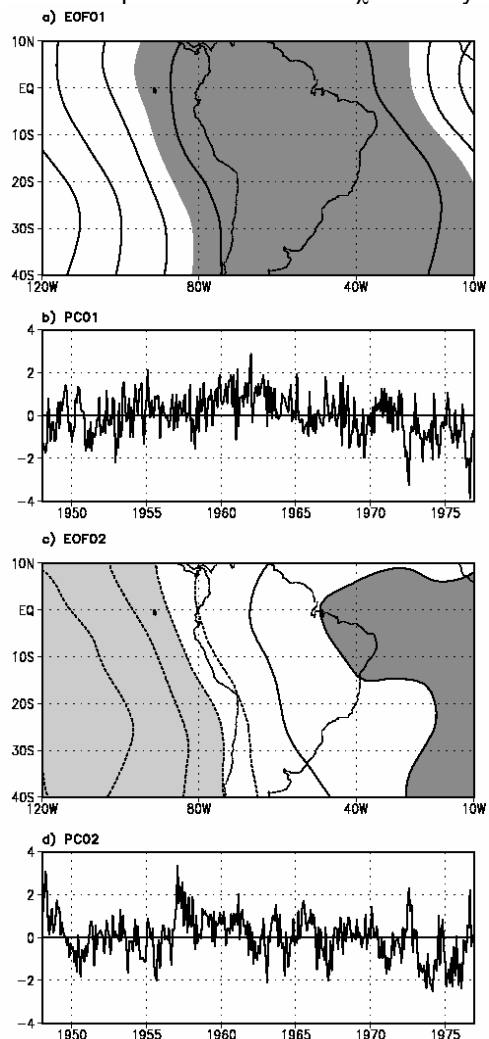


Figure 1 – Loading patterns and PC of the first two EOF modes of the transient- χ for 1948-1976. Contour interval is 0.20. The zero contour has been omitted. Light (Dark) shading area indicates values less (greater) than -0.7 (0.7) in (a) and than -0.4 (0.4) in (c).

The EOF01 and EOF02 of the analysis for 1977-1999 are well separated from each other and explain 55.9% and 22.2% of the total variance of

transient- χ , respectively. The patterns of these modes are similar to those of the corresponding modes of 1948-1976 (Figs. 1a, 1c, 2a and 2c). The PC01 shows positive trend for some sub-periods of the 1977-1999 period superimposed to interannual oscillations. These sub-periods are: 1977-1983, 1984-1987, and 1988-1994 (Fig. 2b) The PC02 shows pronounced interannual oscillations (Fig. 2d). Thus, the EOF02 for 1977-1999 describes ENSO-related variability of the transient- χ field over the South American region (Figs. 2c and 2d).

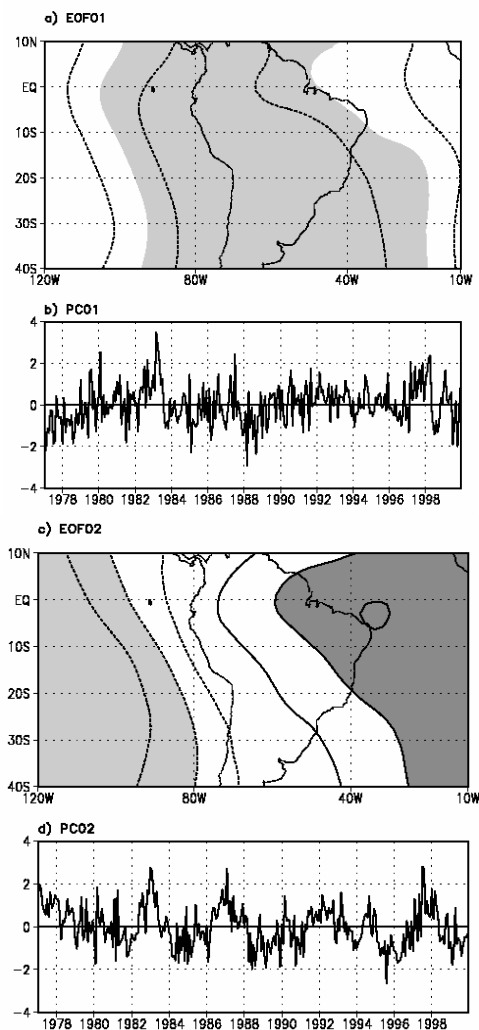


Figure 2 – Loading patterns and PC of the first two EOF modes of the transient- χ for 1977-1999. Display is the same as that in Figure 1.

The EOF01 and EOF02 of the transient- χ anomalies for 1948-1999 are well separated from each other and explain 61.6% and 23.3% of the total variance for this variable, respectively. The

EOF01 shows a similar pattern of that noted for the first modes of the partial periods. For positive (negative) PC01, divergence (convergence) prevails over SA (Figs. 3a and 3b).

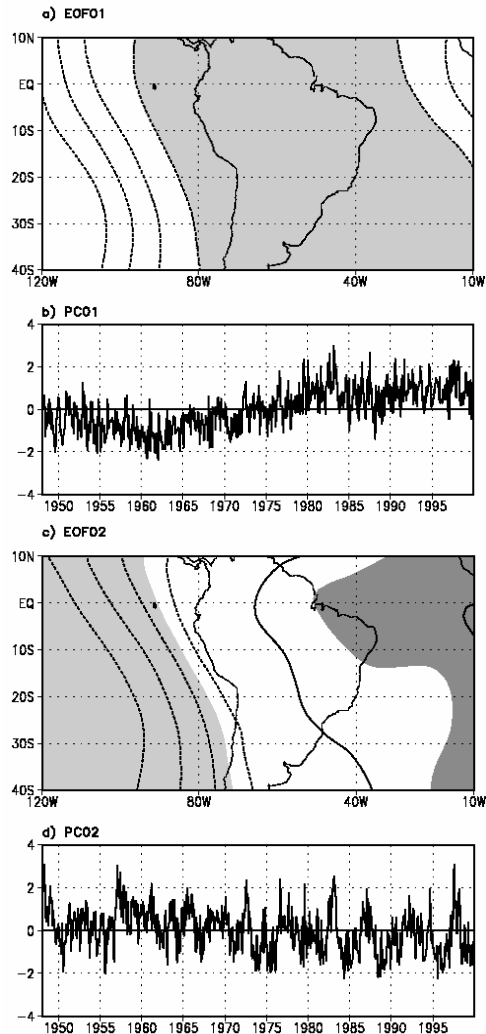


Figure 3 – Loading patterns and PC of the first two EOF modes of the transient- χ for 1948-1999. Contour interval is 0.20. The zero contour has been omitted. Light (Dark) shading area indicates values less (greater) than -0.8 (0.8) in (a) than -0.3 (0.3) in (c).

The PC01 (Fig. 3b) shows a sign reversal from negative to positive by the middle of the 1970's. This PC01 sign reversal is consistent with the PDO phase change by the middle of 1970's (Mantua et al., 1997). The correlations between PC01 of the partial periods and the PC01 of the total period are -0.96 and 0.93 , respectively for 1948-1976 and 1977-1999. So, the EOF01 describes the upper level monsoon divergent

circulation manifesting in an interannual to multi-decadal timescales. The EOF02 also shows a similar pattern of that noted for the second modes of the previous analyses for partial periods, with reversed sign loadings over eastern tropical Pacific (negative) and in the area including northeastern Brazil and tropical Atlantic (positive) (Fig. 3c). The corresponding PC time series shows interannual oscillations with periods approximately of 4-5 years (Fig. 3d). The correlations between PC02 of the partial periods and the PC02 of the total period are 0.97 and 0.86, respectively for 1948-1976 and 1977-1999.

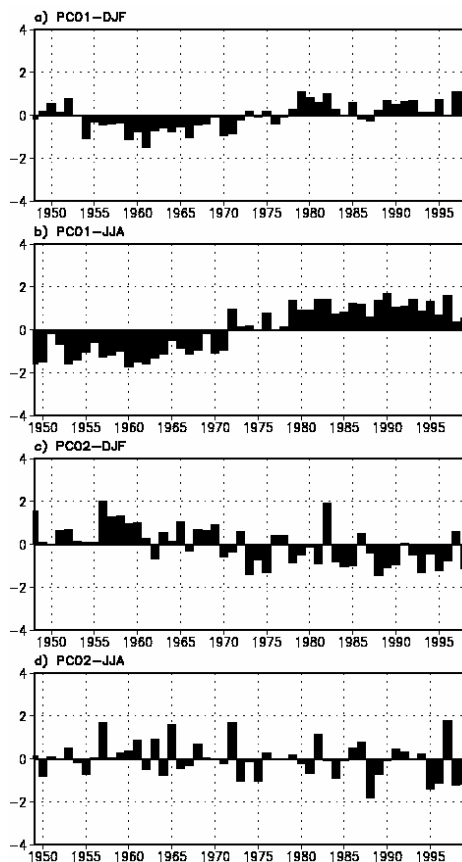


Figure 4 – PC01 and PC02 time series averaged for DJF and JJA months.

The seasonal PC values are obtained for the first two modes of the EOF analysis of 1948-1999 by averaging for DJF and JJA months (Fig. 4). Summer PC01 shows quite small magnitudes before 1953, negative values from 1954 to 1972 and positive values from 1973 onwards (Fig. 4a). Winter PC01 values are negative before 1971, and positive from 1972 onwards (Fig. 4b). The seasonal PC01 also shows interannual variability

superimposed to multidecadal variability. Summer PC02 displays alternating signs at 1-3 year timescale during 1961-1980, predominantly positive values before 1960 and negative values from 1981 onwards (Fig. 4c). Thus, summer PC02 contains interannual and decadal timescale variations. Winter PC02 shows well defined interannual fluctuations with most positive (negative) values occurring during the onset years of El Niño (La Niña) events of: 1957, 1965, 1972, 1977, 1982, 1987, 1991, 1994 e 1997 (1950, 1955, 1964, 1970, 1973, 1975, 1988 e 1998). The El Niño and La Niña years were obtained at <http://ggweather.com/enso/years.htm>.

3.2 Composites

Table 1 lists the years used in the composites. Years with $PC01 < -0.5$ ($PC01 > 0.5$) are within the 1948-1976 (1977-1999) when the negative (positive) PDO phase occurred. The years listed for DJF composites refer to December.

Table 1 – Years used in the composites

	DJF	JJA
PC < -0.5	1954, 1956, 1959, 1960, 1961, 1962, 1963, 1964, 1965, 1966, 1970, 1971	1949, 1950, 1952, 1953, 1954, 1955, 1956, 1957, 1958, 1959, 1960, 1961, 1962, 1963, 1964, 1966, 1967, 1968, 1970, 1971
PC > 0.5	1979, 1980, 1981, 1982, 1985, 1989, 1990, 1991, 1992, 1995, 1997, 1998	1979, 1980, 1981, 1982, 1983, 1984, 1985, 1986, 1987, 1988, 1989, 1990, 1991, 1992, 1993, 1994, 1995, 1996, 1997, 1999

3.2.1 Summer composites

The negative composite of SST anomalies (SSTAs) shows significant negative values in the tropical Indian and Pacific Oceans and in the oceanic areas to the south of 40°S, and positive ones in the North Atlantic (Fig. 5a). The positive

composite holds a nearly reversed sign pattern (Fig. 5f). These composites are quite similar to the SSTA pattern of the PDO mode described by Mantua et al. (1997).

Coherently, the negative (positive) composites of the surface air temperature show negative (positive) anomalies overlying the tropical oceanic regions with negative (positive) SSTAs, over the equatorial and tropical South Atlantic, and over most of SA and equatorial Africa (Figs. 5b and 5g). In addition, for the positive composite, positive anomalies are also found over China and eastern Asia.

The negative (positive) composite of SLP anomalies (SLPAs) exhibits a strong zonal structure with negative (positive) values in the tropics between 30°W and 180°W and opposite sign SLPAs over North Pacific, North Asia and Russia (Figs. 5c and 5h). For the negative composite, the positive SLPAs over northeastern Brazil are coherent with the presence of negative anomalies of surface air temperature.

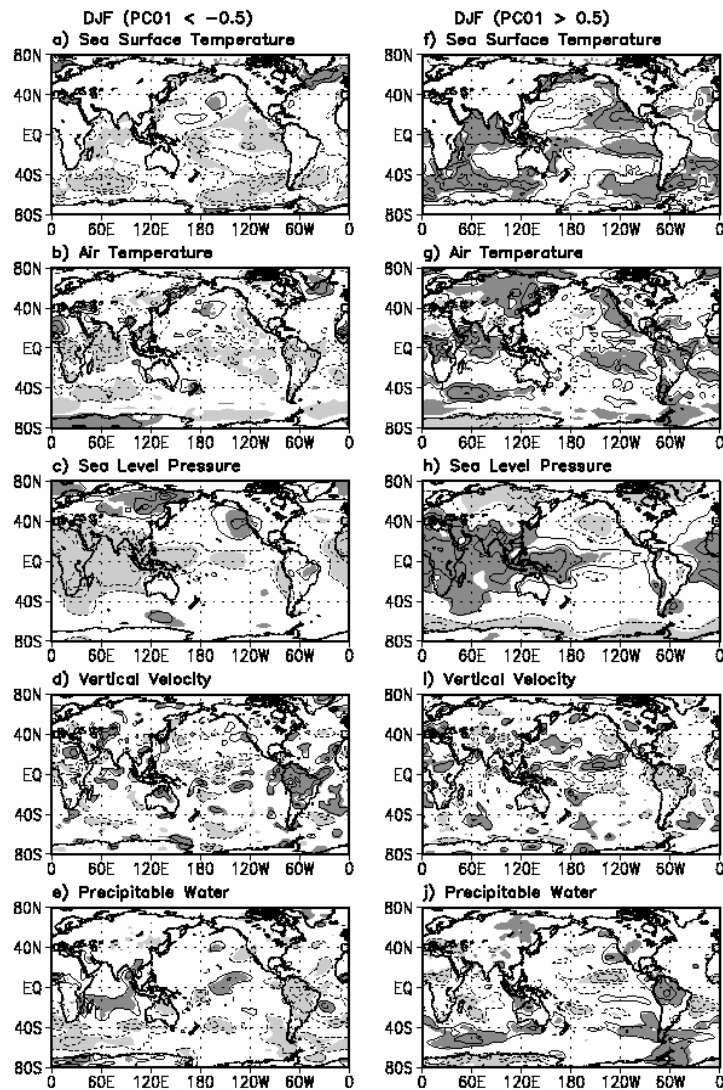


Figure 5 – DJF anomaly composites of SST, surface air temperature, SLP, vertical velocity and precipitable water for $PC01 < -0.5\sigma$ (a, b, c, d and e), and for $PC01 > 0.5\sigma$ (f, g, h, i and j). Contour interval is 0.3σ , with negative (positive) contours being dashed (continuous). The zero contour has been omitted. Shading area encompasses significant values.

Similar to the composites for the other variables, the negative and the positive composites of the 500 hPa vertical velocity show nearly reversed sign patterns. The negative anomaly composite of the 500 hPa vertical velocity shows sinking motions over most of tropical SA and surrounding oceanic areas and rising motions over the central Pacific along 10°N (Fig. 5d), which are consistent respectively with positive and negative SLPAs in these regions. The positive composite of the 500 hPa vertical velocity holds nearly reversed patterns (Fig. 5i).

The PW composites show very coherent patterns with enhanced (suppressed) PW

occurring in the areas with anomalous upward (downward) motions (Figs. 5d, 5i, 5e and 5j).

3.2.2 Winter composites

Winter composites present smoother and broader patterns when compared with those of summer composites. The negative composite of the SSTAs features negative values in most of the Indian Ocean, eastern Pacific, equatorial Atlantic and tropical South Atlantic, and positive values in central North Pacific and North Atlantic (Fig. 6a). The positive SSTAs composite shows similar

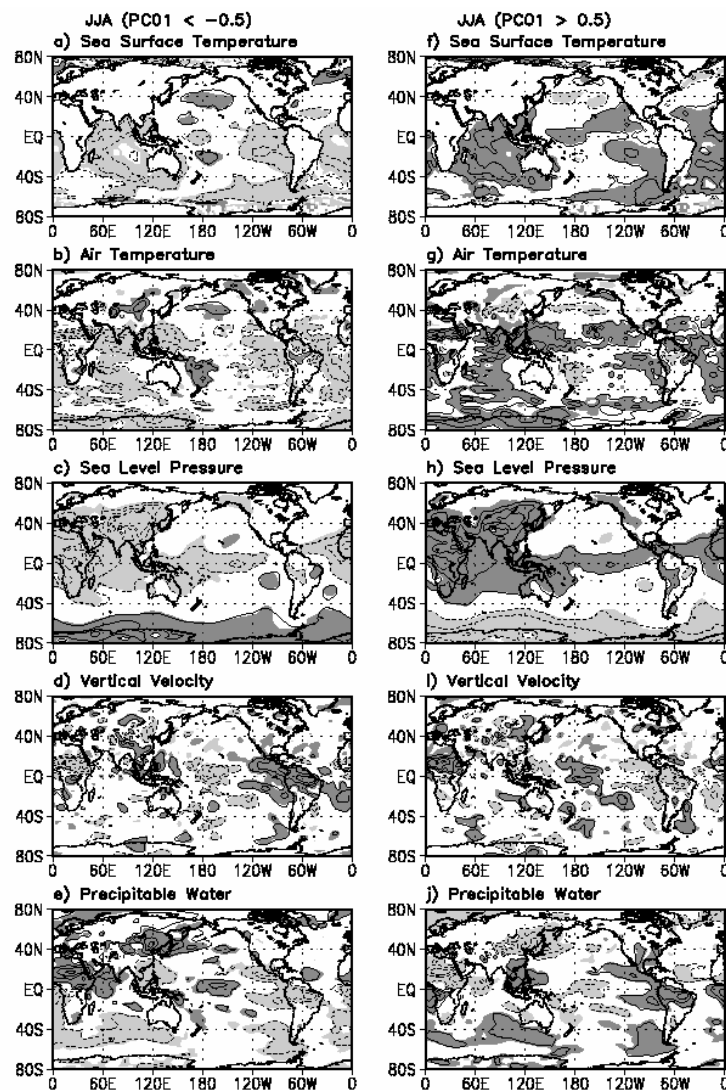


Figure 6 – JJA anomaly composites of SST, surface air temperature, SLP, vertical velocity and precipitable water for PC01 < -0.5σ (a, b, c, d and e) and for PC01 > 0.5σ (f, g, h, i and j). Contour interval is 0.3 σ, with negative (positive) ones being dashed (continuous). The zero contour has been omitted. Shading area encompasses significant values.

reversed sign pattern, except that a zonal area with positive SSTAs is found in the central Pacific (Fig. 6f).

Consistently, the negative (positive) composite of the surface air temperature shows negative (positive) values over the regions with negative (positive) SSTAs and over the northeastern SA, India, Indonesia and in part of Africa, and opposite sign anomalies over Mongolia and southwestern Amazon (Figs. 6b and 6g).

The corresponding SLPA composites feature strong zonal structure with significant negative (positive) values in the tropics between the 30°W and 120°E and along the central equatorial Pacific (Figs. 6c and 6h). The negative (positive) composite shows the strongest SLPAs over China, where warmer (cooler) than average surface air prevails (Figs. 6c, 6h, 6b and 6g). The significant positive (negative) SLPAs over northeastern SA are consistent with below (above) normal surface air temperature noted for the corresponding negative (positive) composites.

The composites of 500 hPa vertical velocity and PW are consistent and feature a zonal wave number two structure for these variables along the equatorial latitudes. Positive (negative) PW anomalies (PWAs) coincide with the region of ascending (descending) motions (Figs. 6d, 6e, 6i and 6j). For the negative composite, the anomalous ascending motions over tropical north Africa and central equatorial Pacific are compensated by anomalous descending motions over western equatorial Pacific and over the extensive area including eastern equatorial Pacific, northern SA and tropical South Atlantic. The positive composite of the vertical velocity anomalies holds a nearly reversed sign pattern.

4. CONCLUDING REMARKS

The first EOF modes of the 1948-1976 and 1977-1999 periods show similar patterns and describe interannual variability superimposed to decadal variability of the SAMS. The EOF02 modes for these periods describe ENSO-related SAMS variability.

The EOF01 modes of the total and partial periods are quite similar. Further the PC01 of the partial periods and PC01 of the total period show correlations of -0.96 and 0.93, respectively for 1948-1976 and 1977-1999. Therefore, the EOF01 of the total period describes interannual, decadal and multidecadal variability of the SAMS. The anomaly composite for SST related to this mode shows a pattern similar to that found in previous work for the PDO (Mantua et al., 1997). The

associated anomaly composites for the reanalyzed variables show consistent patterns over SA. An important aspect revealed by the PW composites is that the SAMS weakened before 1976 and enhanced afterwards. The long-term variability of the SAMS might be related to the PDO.

5. REFERENCES

- Andreoli, R. V., and M. T. Kayano, 2005: ENSO-related rainfall anomalies in South America and associated circulation features during warm and cold Pacific Decadal Oscillation regimes. *Int. J. Climatol.*, **25**, 2017-2030.
- Chu, P.-S., Z.-P. Yu, and S. Hastenrath, 1994: Detecting climate change concurrent with deforestation in the Amazon Basin: Which way has it gone? *Bull. Amer. Meteorol. Soc.* **75**: 579-583.
- Grimm, A. M., C. S. Vera, and C. R. Mechoso, 2004: The South American Monsoon System. WMO, The Third International Workshop on Monsoons, Hangzhou, China, 2-6 November, 111-129.
- Kalnay, E. and co-authors 1996: The NCEP/NCAR 40-year Reanalysis Project. *Bull. Amer. Meteorol. Soc.*, **77**, 437-471.
- Mantua, N. J., S. R. Hare, Y. Zhang, J. M. Wallace, and R. C. Francis, 1997: A Pacific interdecadal climate oscillation with impacts on salmon production. *Bull. Amer. Meteorol. Soc.*, **78**, 1069-1079.
- North, G. R., T. L. Bell, R. F. Cahalan, and F. J. Moeng, 1982: Sampling errors in the estimation of empirical orthogonal function. *Mon. Wea. Rev.*, **110**, 699-706.
- Smith, T. M., and R. W. Reynolds, 2003: Extended reconstruction of global sea surface temperatures based on COADS data (1854-1997). *J. Clim.*, **16**, 1495-1510.
- Tanaka, H. L., N. Ishizaki, and A. Kitoh, 2004: Trend and interannual variability of Walker, monsoon and Hadley circulations defined by velocity potential in the upper troposphere. *Tellus*, **56A**, 250-269.
- Vera, C. W. Higgins, J. Amador, T. Ambrizzi, R. Garreaud, D. Gochis, D. D. Lettenmaier, J. Marengo, C. R. Mechoso, J. Nogués-Paegle,; P. L. da Silva Dias, and C. Zhang, 2005: A unified view of the American Monsoon Systems. Accepted in *J. Clim.* special issue for the 1st CLIVAR Science Conference.
- Zhou, J.Y., and W. K.-M Lau, 2001: Principal modes of interannual and decadal variability of summer rainfall over South America. *Int. J. Climatol.*, **21**, 1632-1644.